PART

II Nuclear structure

5 The two-body system

The simplest complex nucleus is the deuteron (^2H), the bound state of the neutron–proton system. Because of its structural simplicity, it provides little guidance to the understanding of the average nucleus of, say, $A = 100$. The two-body system, however, does give information on the nucleon–nucleon force, which is an example of the strong (hadronic) interaction, and this force must provide the major stabilizing influence in nuclear matter. The properties of infinite nuclear matter, from which optimistically one may hope to understand some of those of finite nuclei, will be outlined in Chapter 6; the present chapter is concerned only with information available from a study of the neutron–proton and proton–proton interactions (Ref. 5.1).

5.1 General nature of the force between nucleons

From the fact that complex nuclei exist, the force must be *attractive*, and sufficiently strong to overcome the repulsion of the Z protons contained within the nuclear volume (according to the neutron–proton model). The *range* was indicated crudely by the early α-particle scattering experiments, which showed deviations of the force from pure Coulomb repulsion for light nuclei at distances of approach of the order of a nuclear radius, say, 4×10^{-15} m. A closer estimate was obtained by Wigner from a consideration of the stability of the simple nuclei ^2H, ^3H and ^4He.

Extension of Wigner's calculations led to the difficulty that an assembly of nucleons interacting attractively by a short-range force would collapse to a size of the order of the force range. The total potential energy of a nucleus containing A nucleons would then increase roughly as the number of interacting pairs, i.e. proportionally to A^2, whereas the evidence of mass measurements (Ch. 6) is that the total binding energy varies only as A.

It therefore becomes necessary to postulate a force that provides *saturation*, i.e. that limits the number of attractive interactions within the nucleus.

One way of ensuring saturation is to assume that the potential energy V of a pair of nucleons has the form shown in Fig. 5.1, analogous in radial variation to that describing van der Waals' forces between molecules. Such a potential indicates an attractive force $F=-\partial V/\partial r$ at extreme range and a repulsive force at very short distances. If the interparticle distance at the potential minimum $V=-V_0$ is r, then according to the uncertainty principle the particles must have a relative momentum of the order of $\hbar/r$. The corresponding kinetic energy is $\frac{1}{2}(\hbar^2/\mu r^2)$ where μ is the reduced mass of the system, assuming non-relativistic motion. If

$$V_0 > \tfrac{1}{2}(\hbar^2/\mu r^2) \tag{5.1a}$$

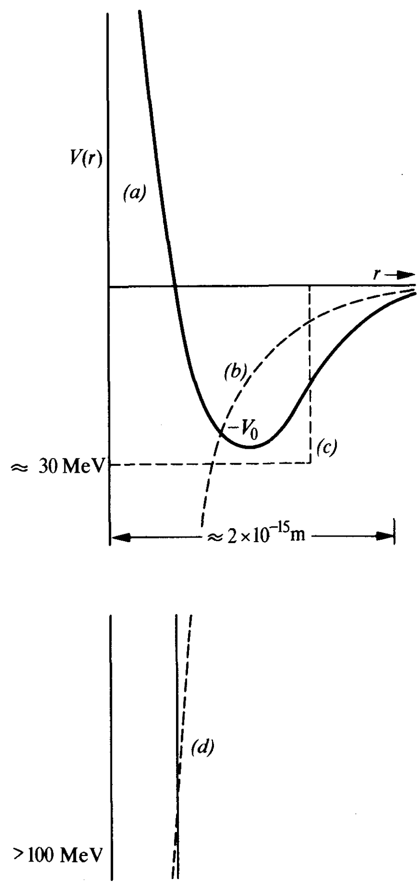

Fig. 5.1 The internucleon potential: (*a*) Schematic, showing repulsive core. (*b*) Form of Yukawa potential. (*c*) Square-well potential. (*d*) Well depth with sharp hard core.

a bound state may be formed, with a negative discrete energy. If, however,

$$V_0 < \tfrac{1}{2}(\hbar^2/\mu r^2) \tag{5.1b}$$

the total energy of the system lies in the continuum and the interaction is a scattering process.

The existence of a repulsive core creates difficulties in nuclear matter calculations. It is therefore usual, at least for problems concerned only with low relative momentum, to approximate the potential by simple spherically symmetrical forms with a suitable long-range behaviour, e.g. the *square-well potential:*

$$V = -V_0 \quad \text{for} \quad r < R \tag{5.2}$$

or the *Yukawa potential:*

$$V = -V_0 \exp(-r/R)/(r/R) \tag{5.3}$$

or the oscillator potential (Sect. 1.4.2). The potentials (5.2) and (5.3) are sketched in Fig. 5.1.

The depth of the potential well depends on the nature of the repulsive core. For nucleons interacting in free space through a Yukawa-type potential with a sharp hard-core radius of 0·5 fm the well depth obtained phenomenologically varies between 100 and 1000 MeV for the main attractive central part of the potential. In complex nuclei, however, observed nuclear densities (Ch. 6) show that the average spacing between nucleons is about 1·8 fm and at this separation the force is much weaker. In discussions of the nucleon–nucleon system at low energies and of the average potential in nuclei (Ch. 7) it will be convenient to use a simple square-well approximation, with a range of 1·5–2 fm and a depth of 30–60 MeV.

5.2 The scattering of neutrons by protons

5.2.1 Experimental

Because of the absence of Coulomb scattering the neutron–proton nuclear interaction can be studied with reactor neutron beams at sub-thermal energies. It can also be followed through the MeV region to the highest energies available for secondary particles from proton accelerators. Throughout this extensive range of energies, total cross-sections (Sect. 1.2.5) are observable by simple attenuation methods using hydrogen targets and the results obtained are shown in Fig. 5.2. The rise in cross-section below the energy 1 eV occurs because at these energies the two protons in the hydrogen molecule can no longer be treated as free, or independent. When these effects are corrected for it is found that the neutron-free proton total cross-section is approximately constant at about 20·4 b over a range of several hundred electron volts in energy.

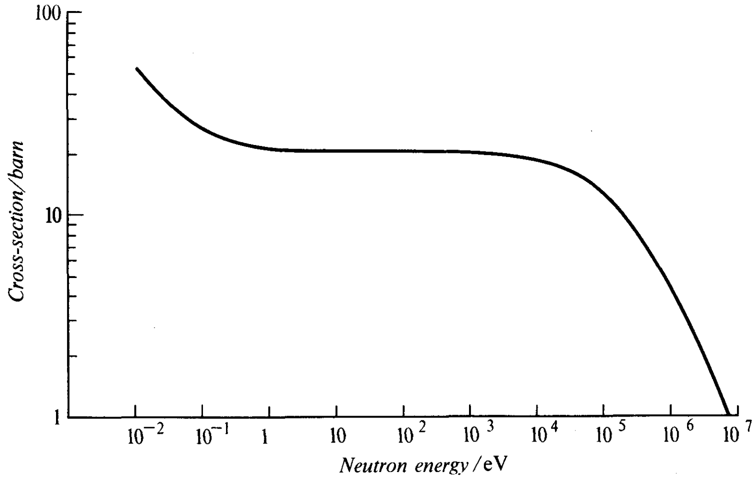

Fig. 5.2 Total cross-section for neutron–proton interaction, measured by attenuation methods, as a function of laboratory neutron energy.

In accordance with the arguments presented in Section 1.2.6, a principal effect of increasing the energy of neutrons interacting with protons is to introduce additional partial waves. Although this alters the integrated cross-section it is more directly observable in the angular distribution of scattering, at least at energies for which more than s-waves ($l = 0$) are involved. Figure 5.3 shows the centre-of-mass angular distribution of neutrons of a number of energies scattered by protons.

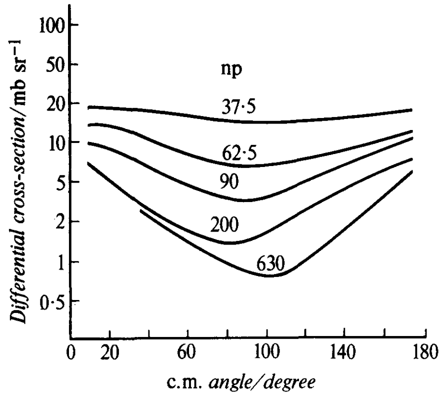

Fig. 5.3 Differential cross-section for neutron–proton scattering. The laboratory neutron energies in MeV are shown on the curves. At large angles in the c.m. system the proton takes most of the incident neutron energy and the process is then described as *charge-exchange scattering* (Lock, W. O. and Measday, D. F., *Intermediate Energy Nuclear Physics*, Methuen, 1970).

From the angular distribution and total cross-section data, phase shifts for the different partial waves as a function of energy may be extracted. These form both a convenient representation of the experimental results and a starting point for a theoretical analysis in terms of potentials. Figure 5.4 gives the phase shift curve for the neutron–proton system in the states $^1S_0$ (spins of neutron and proton opposed) and $^3S_1$ (spins parallel). The way in which these two states of motion are distinguished experimentally will now be described. A brief discussion of the high-energy data will be found in Section 5.6.2.

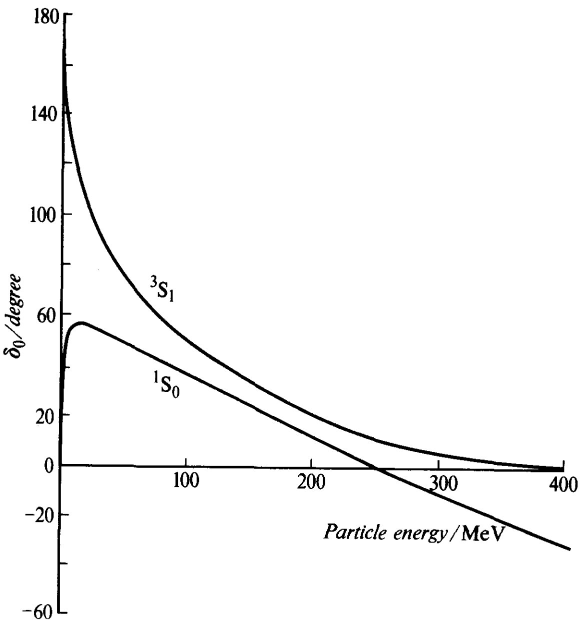

Fig. 5.4 The s-wave phase shifts δ_0 for the neutron–proton interaction (schematic). The curves embody observations on proton–proton scattering.

5.2.2 *Description of low-energy* (np) *scattering*

Low-energy scattering will be taken to refer to energies for which only s-waves, with zero orbital angular momentum in the c.m. system, need be considered and non-relativistic formulae are usually adequate. If the neutron and proton are assumed to have equal mass M, then the reduced mass of the interacting system (for the equivalent single-particle problem) is

$$\mu = M/2 \tag{5.4}$$

and the wavenumber k of the relative motion, for a laboratory neutron energy T_n is given by setting the c.m. energy $\frac{1}{2}T_n$ equal to $\hbar^2k^2/2\mu$, the non-relativistic expression for momentum k. This gives

$$k^2 = (2\mu/\hbar^2)\tfrac{1}{2}T_n \tag{5.5}$$

For neutrons of energy 1 MeV the reduced de Broglie wavelength is $ƛ = 1/k = 9{\cdot}1 \times 10^{-15}$ m and as this is very much greater than the expected range of nuclear forces the assumption of s-wave interaction is justified for this energy, and will be assumed valid up to, say, $T_n = 10$ MeV.

The only inelastic reaction possible between neutrons of energy $1-10$ MeV and free protons is the capture reaction

$$\mathrm{n}+\mathrm{p} \rightarrow \mathrm{d}+\gamma \tag{5.6}$$

and experimentally this has a cross-section of less than 1 per cent of the scattering cross-section, so that it may be disregarded for present purposes. The total cross-section is then equal to the integrated elastic scattering cross-section.

Following now the general treatment of elastic scattering given in Section 1.2.7, we represent the region of interaction by a spherically symmetrical potential well of depth V_0 and radius R. The incident neutron wave is an s-state solution of the free-space Schrödinger equation and this, from equations (1.69) and (1.71), has the form (valid for all kr)

$$u_i(r) = r\psi_i(r) = (A/k)\sin kr \tag{5.7}$$

Similarly, the final wave may be taken to be the s-wave part of equation (1.72), with $\eta = 1$ for elastic scattering, namely

$$u_f(r) = r\psi_f(r) = (A\exp(i\delta_0)/k)\sin(kr+\delta_0) \tag{5.8}$$

which shows the phase shift δ_0 due to the interaction. This is positive for an attractive potential (Sect. 1.2.7). The integrated elastic scattering cross-section is given by

$$\sigma_{\mathrm{el}}^0 = (4\pi/k^2)\sin^2\delta_0 \tag{5.9}$$

from equation (1.80), and a measurement of σ_{el}^0 gives δ_0.

To relate δ_0 to the parameters of the potential well we impose the condition of continuity of the final wavefunction and its derivative at the boundary $r = R$ at which the wavenumber changes since the Schrödinger equation for $r < R$ contains the potential V_0. In this region, the $l = 0$ solution is

$$u = r\psi(r) = (B/K)\sin Kr \tag{5.10}$$

where

$$K^2 = (2\mu/\hbar^2)(V_0 + \tfrac{1}{2}T_n) = 2\mu V_0/\hbar^2 + k^2 \tag{5.11}$$

The continuity condition, expressed in terms of a useful dimensionless parameter ρ, then gives

$$\rho = \left(\frac{r}{u}\frac{\mathrm{d}u}{\mathrm{d}r}\right)_{r=R} = KR \cot KR = kR \cot(kR+\delta_0) \tag{5.12}$$

If $k \ll K$, which means physically that the incident energy T_n is much less than the depth of the potential well, this equation shows that the phase shift is determined by the well parameters.

It is instructive to proceed with the evaluation of δ_0 in the *low-energy limit* $k \to 0$, assuming that the cross-section remains constant, so that equation (5.9) requires that in the limit $\sin\delta_0/k$ shall remain finite. From equation (5.12)

$$(1/k)\tan(kR+\delta_0) = R/\rho \tag{5.13}$$

so that as $k \to 0$

$$R + \tan\delta_0/k = R/\rho \tag{5.14}$$

or

$$\tan\delta_0/k = -R(1-1/\rho) = -a(k) \tag{5.15}$$

In the limit $k=0$, $a(k)=a$ is defined to be the *scattering length*; it is also equal in absolute magnitude, for $\delta_0 \approx \tan\delta_0$, to the s-wave *scattering amplitude* given by equation (1.77) so that it then has the physical interpretation that it is the amplitude of the wave *scattered* by the potential well for unit incident amplitude. The scattering length, as defined by equation (5.15), is shown in Fig. 5.5*a* in the case that the internal wavefunction $\sin Kr$ just turns over within the distance R, i.e. $KR \geq \pi/2$. It will be seen in Section 5.2.3 that this is also the condition for the existence of a *bound state*, in fact the deuteron. If the neutron and proton collide with parallel spins, the scattering state will be a state of the same potential well as binds the deuteron, i.e. a $^3S_1$ (triplet) state orthogonal to the ^3S bound state. The figure makes it clear that as $k \to 0$ the phase shift δ_0 given by

$$\tan\delta_0 = -ka \tag{5.16}$$

tends to π.

There is, of course, a further scattering state, the $^1S_0$ (singlet) state, in which the neutron and proton collide with spins opposed. This is not known as a stable state of the deuteron and will involve a different potential well. The scattering length in this case is shown in Fig. 5.5*b*, which indicates a wavefunction *rising* at the potential boundary so that only scattering states exist. The internal wavefunction does *not* turn over in the radial distance R and $KR \leq \pi/2$, owing to a shallower singlet potential well. The scattering length is negative and the phase shift, given by equation (5.16), tends to zero as $k \to 0$.

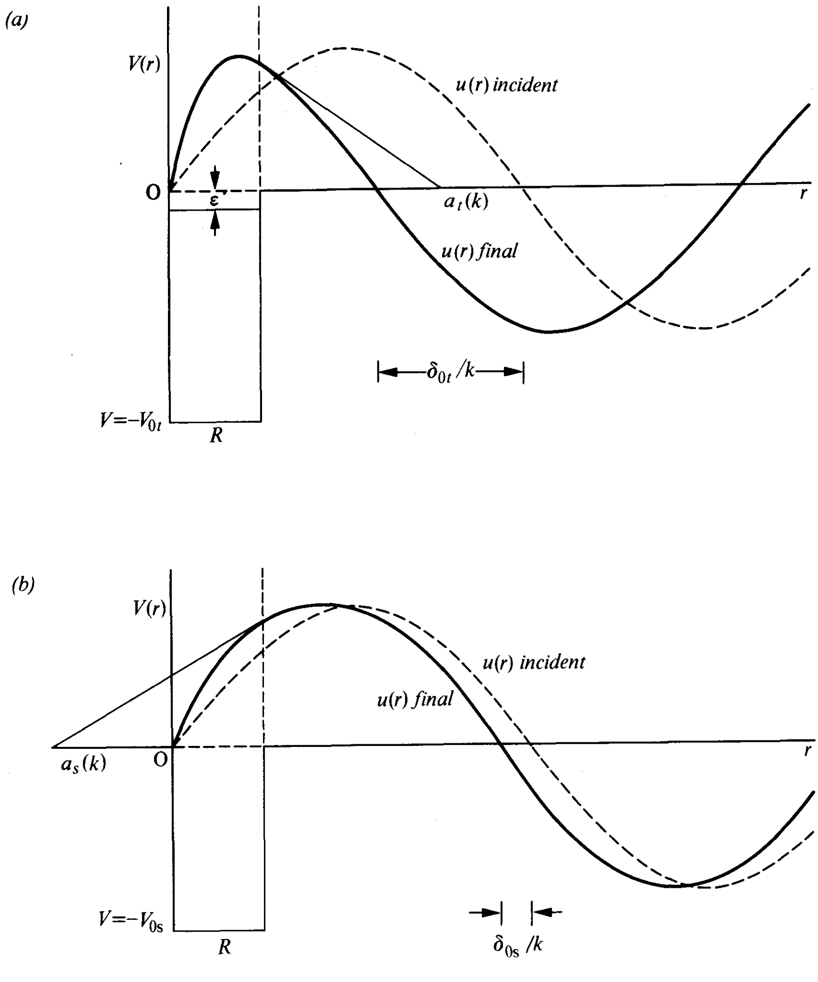

Fig. 5.5 Neutron–proton scattering at low energy, showing wave amplitudes, phase shifts and scattering lengths in relation to the square-well potential for (*a*) triplet (^3S) state, (*b*) singlet (^1S) state. In the triplet case the binding energy ε of the deuteron is indicated.

The special case of a bound state at zero energy is found for $KR = \pi/2$, or $(2n+1)\pi/2$, and gives $\rho = 0$. From Fig. 5.5, the scattering length then becomes infinite and $\delta_0 = (n+\frac{1}{2})\pi$. This is an example of *resonance scattering*.

In all three cases the scattering cross-section at zero energy in the present approximation is given by equations (5.9) and (5.15) as $\sigma^0_{el} = 4\pi a^2$.

In a collision between unpolarized neutrons and protons, there are four possible combinations of the two intrinsic spins of $\frac{1}{2}\hbar$; of these, three belong to the triplet state $^3S_1$ and one to the singlet $^1S_0$. The relative weights of these two states are, therefore $\frac{3}{4}$ and $\frac{1}{4}$. Using these factors and denoting the triplet and singlet scattering lengths by a_t, a_s the cross-section for elastic scattering may be written, using (5.9) and (5.15),

$$\begin{aligned}\sigma_{\text{el}}^0 &= (4\pi/k^2)[\tfrac{3}{4}\sin^2\delta_{0t}+\tfrac{1}{4}\sin^2\delta_{0s}]\\ &= (4\pi/k^2)\left[\frac{3}{4(1+\cot^2\delta_{0t})}+\frac{1}{4(1+\cot^2\delta_{0s})}\right]\\ &= \pi[3/(k^2+1/a_t^2)+1/(k^2+1/a_s^2)] \qquad (5.17)\end{aligned}$$

For $k\approx 0$ the cross-section becomes

$$\sigma_{\text{el}}^0=\pi(3a_t^2+a_s^2) \qquad (5.18)$$

and this near-zero-energy cross-section of 20·4 b is one of the basic observables for the two-body system.

For higher energies there is some energy dependence in the cross-section and it is useful to expand the inverse scattering length $1/a$ as a power series in k^2, which gives

$$k\cot\delta_0=-1/a+\tfrac{1}{2}r_0k^2\cdots \qquad (5.19)$$

where the coefficient r_0 is known as the *effective range* and corresponds physically (Appendix 3) with an average distance of interaction between the neutron and proton. It also depends on the well depth, but not on its shape, and formula (5.19) taken as far as the k^2 term applies in the *shape-independent approximation.* It is the validity of this approximation (Appendix 3) that justifies the use of the simple square well for discussion of the s-wave (np) interaction. The cross-section in this approximation becomes

$$\sigma_{\text{el}}^0=\pi\{3/[k^2+(1/a_t-\tfrac{1}{2}r_{0t}k^2)^2]+1/[k^2+(1/a_s-\tfrac{1}{2}r_{0s}k^2)^2]\} \qquad (5.20)$$

and this formula has been applied to analyse scattering data up to about 10 MeV incident neutron energy.

The necessity for both singlet and triplet scattering amplitudes in low-energy (np) scattering was first pointed out by Wigner, when it had become clear that the triplet amplitude alone, as predicted from the binding energy of the deuteron (Sect. 5.2.3) led to a cross-section of only about 2 b compared with the observed 20·4 b. This is clear evidence for the *spin-dependence* of the interaction potential.

5.2.3 *The bound state (the deuteron)*

The deuteron has a binding energy of 2·2245 ± 0·0002 MeV and no stable excited states. It has an angular momentum of $1\hbar$ and both a magnetic dipole moment μ_d and an electric quadrupole moment. The magnetic moment is not equal to the algebraic sum of the magnetic moments of the proton μ_p and neutron μ_n, but it is sufficiently near to preclude the possibility of relative orbital motion of the two particles in a first approximation. The simplest structure to assume for the ground state of the deuteron is, therefore, a neutron and a proton in an S-state of orbital motion with parallel spins, i.e. a $^3S_1$ state, with even parity. The $^1S_0$ state of the deuteron, in which the proton and neutron have antiparallel spins, is unbound.

It has already been noted that $^3S_1$ and $^1S_0$ states are needed to describe the scattering problem, and the wavefunction for the deuteron (^3S) may easily be obtained by applying the formalism of Section 5.2.2 to the case of a total energy that is negative and equal numerically to the binding energy ε (Fig. 5.6). From the free-space Schrödinger equation for $r > R$,

$$\frac{d^2u}{dr^2} + \left(\frac{2\mu}{\hbar^2}\right)(-\varepsilon)u = 0 \tag{5.21}$$

the solution

$$u(r) = C \exp(-\alpha r) \tag{5.22}$$

where

$$\alpha^2 = 2\mu\varepsilon/\hbar^2 = (0{\cdot}232)^2 \text{ fm}^{-2} \tag{5.23}$$

is obtained after the additional solution $e^{\alpha r}$ has been excluded because of its unphysical behaviour for large r. The quantity $1/\alpha =$ 4·31 fm is a 'size' parameter for the deuteron, measuring the radial extent of the wavefunction (5.22); it is determined by the binding energy ε.

The external wavefunction must join smoothly with the wavefunction for $r < R$, which is a solution of the Schrödinger equation

$$d^2u/dr^2 + (2\mu/\hbar^2)(-\varepsilon + V_0)u = 0 \tag{5.24}$$

and has the form of (5.10), i.e.

$$u(r) = (B/K_d) \sin K_d r \tag{5.25}$$

with

$$K_d^2 = (2\mu/\hbar^2)(V_0 - \varepsilon) \tag{5.26}$$

The necessary boundary condition is

$$\rho/R = (1/u\,.\,du/dr)_{r=R} = K_d \cot K_d R = -\alpha \tag{5.27}$$

from (5.25) and (5.22), and it follows that

$$\cot K_d R = -\alpha/K_d = -[\varepsilon/(V_0 - \varepsilon)]^{1/2} \tag{5.28}$$

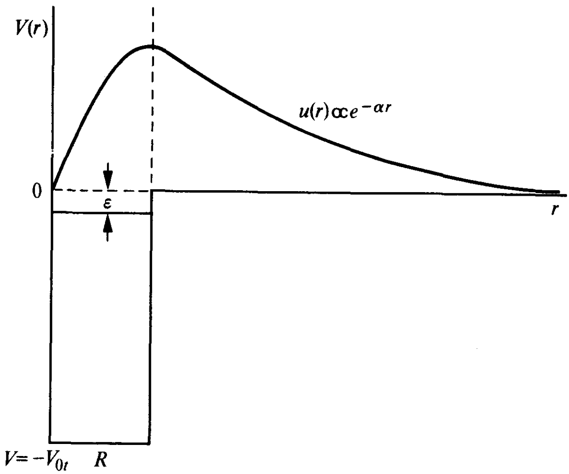

Fig. 5.6 The deuteron wavefunction in relation to the square-well potential.

This is a small quantity so that $K_d R \approx \pi/2$. It could also be $\approx 3\pi/2$, $5\pi/2$, etc., but these wavefunctions would have radial nodes and would not give the state of lowest energy.

Assuming as a first approximation that $K_d R = \pi/2$ it follows that

$$2\mu V_0 R^2/\hbar^2 = \pi^2/4$$

and

$$V_0 R^2 = \pi^2\hbar^2/8\mu = 10^{-28}\,\mathrm{MeV} \times \mathrm{m}^2 \tag{5.29}$$

which is a relation between the *range of the force and the depth of the triplet well.* Equation (5.29) implies that no bound state is possible in the well unless $V_0 R^2 \geqslant \pi^2\hbar^2/8\mu$. The deuteron binding does not appear in (5.29); it is sufficient for the conclusion that a bound deuteron, of small binding energy, exists. Furthermore, so long as $|\varepsilon| \ll V_0$ a relation of the form (5.29) will be obtained whatever the shape of the potential, as already indicated generally in equation (5.1a). Moreover, it may now be seen that for $k=0$ the unbound triplet wavefunction for $r<R$ will be very similar to that of the deuteron (Fig. 5.6) because K becomes equal to K_d if both k and ε are zero.

The triplet scattering length may be connected with the properties of the deuteron by using equations (5.15) and (5.27). These give

$$a_t = R + 1/\alpha \tag{5.30}$$

so that if R is known, a_t determines α, i.e. the binding energy, and conversely. If R is assumed negligible compared with a_t (*zero-range* *approximation*) we obtain from (5.17) a scattering cross-section, assuming only the triplet state,

$$\sigma_{\text{el}}^{0} = 4\pi/(k^2 + 1/a_t^2) = 4\pi/(k^2 + \alpha^2)$$
$$= \frac{2\pi\hbar^2}{\mu} \Big/ (\tfrac{1}{2}T_{\text{n}} + \varepsilon) = 5{\cdot}2/(\tfrac{1}{2}T_{\text{n}} + \varepsilon) \times 10^{-28}\ \text{m}^2 \quad (5.31)$$

where T_{n} and ε are measured in MeV. This is much too small as already observed, and it is not brought into agreement with experiment by using, instead of (5.30), the effective-range formula for a_t, namely (see Ex. (5.4)):

$$1/a_t = \alpha - \tfrac{1}{2}r_{0t}\alpha^2 \qquad (5.32)$$

Only the addition of singlet scattering correctly predicts σ_{el}^{0}.

The triplet scattering length given by the zero-range approximation $a_t = 1/\alpha = \hbar/(2\mu\varepsilon)^{1/2}$ is 4·3 fm. From the total cross-section at zero energy the singlet scattering length is then obtained using equation (5.18) as $|a_s| = 24$ fm. Working back at the present very crude level of approximation it follows that the singlet state of the deuteron should have an energy of $2{\cdot}2 \times (a_t/a_s)^2$ MeV $= 70$ keV although it is not determined whether the state is virtual (unbound) or not. It is likely, however, as shown in Figs. 5.5*a* and 5.5*b*, that the singlet well is shallower than the triplet well. A set of figures, consistent with the evidence so far available, is as follows:

State	*Range of potential*	*Depth of potential*	VR^2
$^3S_1$	$R_t = 1{\cdot}93$ fm	$V_{0t} = 38{\cdot}5$ MeV	1·43 MeV × b
$^1S_0$	$R_s = 2{\cdot}50$ fm	$V_{0s} = 14{\cdot}3$ MeV	0·89 MeV × b

The ranges R are both less than $1/\alpha = 4{\cdot}3$ fm so that there is a high probability of the neutron and proton being separated by more than the range of the force; the 'size' of the deuteron is determined by its binding energy and not by the range. The square-well ranges R are comparable with the reduced Compton wavelength of a pion, $\hbar/m_\pi c = 1{\cdot}42$ fm and with the effective ranges r_0 (Table 5.1).

We now consider the additional information that enables the parameters a_t, a_s, r_{0t}, r_{0s} to be most accurately determined.

5.2.4 *Coherent scattering and the* (np) *parameters*

Further relations between the singlet and triplet scattering parameters and observable cross-sections may be obtained from a study of the interference effects found in the scattering of very slow neutrons by the nuclei of hydrogen molecules or by nuclei bound in solids. For coherent scattering by hydrogen the neutron wavelength must exceed the intermolecular distance 0·078 nm and in fact it must be greater than 0·2 nm (corresponding to $T = 90$ K) if inelastic effects resulting from the conversion of parahydrogen (nuclear spins opposed) to orthohydrogen (spins parallel) are to be avoided. Because of the established spin dependence of the (np) interaction the elastic scattering of neutrons from ortho- and parahydrogen under these long wavelength conditions will differ.

Let the spin vectors divided by $\hbar$ for the neutron and *one* of the hydrogen nuclei of the molecule be s_n, s_p. Then the scattering length for both singlet and triplet collisions may be written

$$a = \tfrac{1}{4}(3a_t + a_s) + (a_t - a_s)\mathbf{s}_n \cdot \mathbf{s}_p \tag{5.33}$$

because for a triplet collision $\mathbf{s}_n \cdot \mathbf{s}_p = \frac{1}{4}$ and for a singlet collision $\mathbf{s}_n \cdot \mathbf{s}_p = -\frac{3}{4}$ as may be seen by inserting eigenvalues in the equation

$$(\mathbf{s}_n + \mathbf{s}_p)^2 = \mathbf{s}_n^2 + \mathbf{s}_p^2 + 2\mathbf{s}_n \cdot \mathbf{s}_p \tag{5.34}$$

For scattering from the *two* protons of the molecule the scattering length is thus

$$a_H = \tfrac{1}{2}(3a_t + a_s) + (a_t - a_s)(\mathbf{s}_n \cdot \boldsymbol{S}_H) \tag{5.35}$$

where $\boldsymbol{S}_H = \mathbf{s}_{p1} + \mathbf{s}_{p2}$ and the assumption of the same phase for the scattering from the two protons is made. The cross-section for elastic scattering is then $\sigma = 4\pi a_H^2$ where

$$a_H^2 = \tfrac{1}{4}(3a_t + a_s)^2 + (3a_t + a_s)(a_t - a_s)\mathbf{s}_n \cdot \mathbf{S}_H + (a_t - a_s)^2(\mathbf{s}_n \cdot \boldsymbol{S}_H)^2 \tag{5.36}$$

The middle term is zero on average if the neutron spin is unaligned and for a similar reason cross-terms in the final bracket vanish, leaving

$$\begin{aligned}(\mathbf{s}_n \cdot \boldsymbol{S}_H)^2 &= s_{nx}^2 S_{Hx}^2 + s_{ny}^2 S_{Hy}^2 + s_{nz}^2 S_{Hz}^2 \\ &= \tfrac{1}{4}\boldsymbol{S}_H^2 \text{ (since } s_{nx} = \tfrac{1}{2}) = \tfrac{1}{4}S_H(S_H + 1)\end{aligned} \tag{5.37}$$

and this has the value 0 for a singlet and $\frac{1}{2}$ for a triplet state. The parahydrogen cross-section is, therefore

$$\sigma_{para} = \pi(3a_t + a_s)^2 \tag{5.38}$$

and the orthohydrogen cross-section

$$\sigma_{ortho} = \pi(3a_t + a_s)^2 + 2\pi(a_t - a_s)^2 \tag{5.39}$$

Experimentally, $\sigma_{para} \approx 4$ b and $\sigma_{ortho} \approx 130$ b for neutrons of energy about 1 mV so that it is immediately apparent that a_s must be large and negative, as has already been indicated for an unbound state, i.e. the singlet state of the deuteron.

The parahydrogen scattering length

$$\tfrac{1}{2}(3a_t + a_s) = 2(\tfrac{3}{4}a_t + \tfrac{1}{4}a_s) \tag{5.40}$$

is double the scattering length $\frac{3}{4}a_t + \frac{1}{4}a_s$ that would be defined for an encounter between a low-energy neutron and a free proton. It is, however, *equal* to the coherent scattering length a_H applicable to the scattering of neutrons by protons bound in crystals. This quantity may be determined accurately by crystal diffraction methods and especially by reflection of thermal neutrons from liquid hydrocarbon mirrors, from which

$$a_H = \tfrac{1}{2}(3a_t + a_s) = -3{\cdot}707 \pm 0{\cdot}008 \text{ fm} \tag{5.41}$$

If this value is combined with the most accurate zero-energy total cross-section

$$\sigma(0) = \pi(3a_t^2 + a_s^2) = 20{\cdot}44 \pm 0{\cdot}23 \text{ b} \tag{5.42}$$

then values for a_t and a_s may be found. The effective-range formula (5.32) and the deuterium binding energy then give r_{0t} and the higher-energy cross-section formula (5.20) then yields r_{0s}. The values of the (np) scattering parameters so found are included in Table 5.1.

5.3 The scattering of protons by protons

5.3.1 Experimental

Because of the Coulomb force between two protons, Rutherford scattering is the predominant interaction at low energies, and the transmission methods used for measuring neutron–proton cross-sections cannot be simply applied, at least at energies of a few MeV or less. On the other hand, the availability of intense beams of particles from accelerators and the convenience of detection methods for charged particles has permitted the accumulation of a very large amount of precise data at all energies up to the limit of accelerator performance. Both total and differential cross-sections are available over the greater part of the energy range since for high energies at least Coulomb effects are chiefly apparent at very small laboratory angles and can be corrected for under simplifying assumptions. The results for cross-section as a function of energy are shown in Fig. 5.7 and some c.m. angular distributions are given in Fig. 5.8.

As with the neutron–proton data, phase shifts may be derived from the differential cross-sections. The Pauli principle eliminates half the states found in the (np) system, e.g. the $^3S_1$ state is forbidden. The phase shifts for the allowed states, e.g. $^1S_0$, are determined to high accuracy for energies for which elastic scattering is the main process of interaction. Above the pion production threshold at about 300 MeV, inelastic reactions are possible and the phase shifts are complex, and less accurate. The $^1S_0$ phase shift has

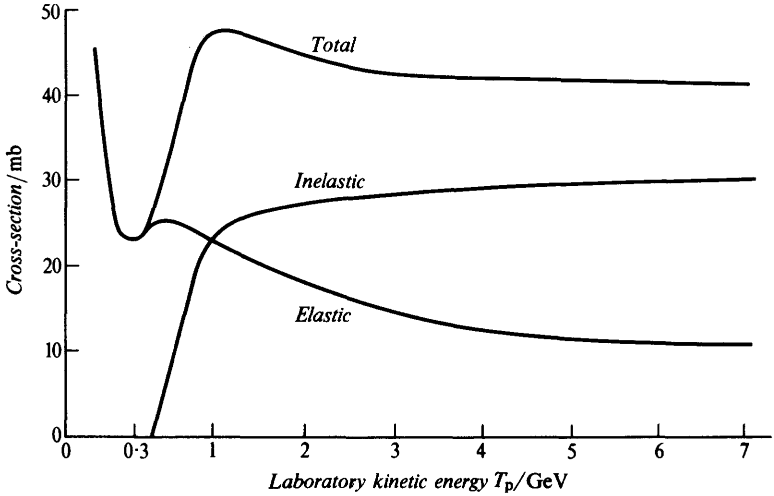

Fig. 5.7 Cross-sections for the proton–proton interaction as a function of energy (plotted on a scale that is linear in momentum). The inelastic cross-section above 0·3 GeV represents meson production.

in fact been presented in Fig. 5.4, since it applies equally to the neutron–proton system (Sect. 5.2) and provides the best singlet scattering information for that system at high energies.

5.3.2 *Description of low-energy* (pp) *scattering*

The Coulomb scattering of identical particles was calculated wave mechanically by Mott. Experimental results confirm the predicted interference at a given angle between waves representing elastically scattered protons and identical recoil particles. This scattering, resulting from a long-range force, involves both singlet and triplet states (i.e. those allowed by the Pauli principle) and all relative orbital momenta. For energies up to approximately 10 MeV, only $^1S_0$ states are allowed for interactions involving the short-range nuclear force although again account must be taken of the identity of the particles.

At energies and angles for which the scattering amplitudes for the Coulomb and nuclear force are comparable, interference effects may be seen, e.g. by the appearance of a minimum in the differential cross-section (Fig. 5.8). The cross-section for scattering involving Coulomb forces and the nuclear s-wave interaction may be written in terms of the corresponding phase shift δ_{0c} as

$$\sigma(\theta) = \sigma_{\mathrm{Mott}}(\theta) - A(\theta, \delta_{0c}) \sin \delta_{0c} + \sin^2 \delta_{0c}/k^2 \qquad (5.43)$$

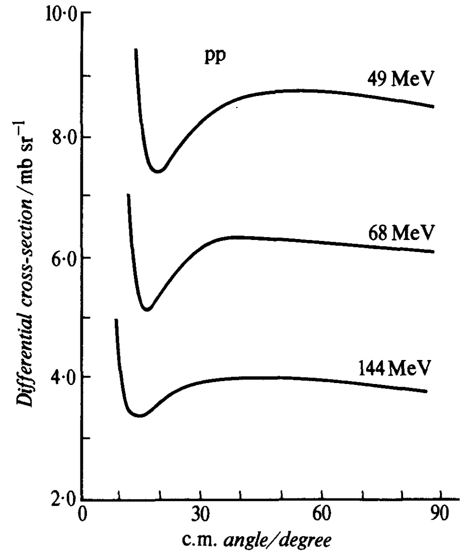

Fig. 5.8 Differential cross-sections for proton–proton scattering showing Coulomb–nuclear interference (Lock, W. O. and Measday, D. F., *Intermediate Energy Nuclear Physics*, Methuen, 1970).

where k is the wavenumber for the relative motion (see eqn (5.5) with $T_n = T_p$) and $A(\theta, \delta_{0c})$ is a calculable coefficient. The last term is the nuclear scattering and the second term is due to Mott–nuclear interference. This term permits the sign as well as the magnitude of δ_{0c} to be found and it is positive, corresponding with an attractive nuclear force.

The effective-range theory used to discuss the (np) interaction has been adapted to describe the variation of the $^1S_0$ phase shift for (pp) scattering with energy. In the shape-independent approximation the formula corresponding to (5.19) is

$$C^2 k \cot \delta_{0c} + (m_p e^2/4\pi\varepsilon_0\hbar^2)h(\eta) = -1/a_s + \tfrac{1}{2}r_{0s}k^2 \qquad (5.44)$$

where

$$C^2 = 2\pi\eta/(\exp 2\pi\eta - 1) \qquad (5.45)$$

is the Coulomb penetration factor and $h(\eta)$ is a calculable function of the *Coulomb parameter* $\eta = e^2/4\pi\varepsilon_0\hbar v$. The factor C^2 appears when a fit is required between internal and external (Coulomb) wavefunctions at the nuclear boundary. In the case of neutron–proton scattering the s-wave phase shift is derived directly from the observed scattering cross-section, but for the proton–proton system δ_{0c} is obtained by analysis of the angular distribution at a number of energies; (5.44) then yields values for the singlet parameters a_s and r_{0s}. The (pp) scattering length a_s is found to be negative, corresponding with an unbound state for the two-proton system, in analogy with the singlet state of the (np) interaction (Fig. 5.5*b*). Recent results are shown in Table 5.1. For comparison with the (np) data, correction must be made for all electromagnetic effects, and a change in the scattering length results, whereas r_{0s} changes only by about 1 per cent.

5.4 The scattering of neutrons by neutrons

The large electromagnetic correction necessary in obtaining a nuclear scattering length from (pp) data justifies consideration of the charge-symmetric (nn) singlet system. Until experiments with colliding beams of neutrons become possible, this requires the study of processes in which two neutrons are left in a final state, e.g.

$$\pi^- + d \rightarrow \gamma + 2n \qquad (5.46a)$$

with stopping pions in which the detailed shape of the energy spectrum of both photons and neutrons depends on the $^1S_0$ (nn) scattering length. Other reactions that have been used are:

$$\left.\begin{aligned} n + d &\rightarrow p + 2n \\ {}^3H + {}^3H &\rightarrow {}^4He + 2n \end{aligned}\right\} \qquad (5.46b)$$

From these, the values for a_s and r_{0s} shown in Table 5.1 have been obtained.

5.5 Comparison of low-energy parameters

Table 5.1 assembles recent results for the reactions so far discussed in the energy region up to 10 MeV. Allowing for the large errors in the (nn) data, and for some uncertainty in corrections to the (pp) scattering length, there is support for the hypothesis of *charge symmetry* between (nn) and (pp) forces in the $^1S_0$ interaction. The (np) singlet scattering length differs substantially from the other two, but this can be accounted for by a very slight difference in the strength of the (np) force, since the $^1S_0$ state is near to zero binding energy and is sensitively dependent on the precise potential that exists (cf. Fig. 5.5*b*). Disregarding this difference, which may arise because charged pions as well as the lighter neutrals can mediate the (np) force (Fig. 2.8) but only neutrals the (nn) and (pp) interaction, it is plausible to assert the *charge independence* of nuclear forces for nucleons in the same state of relative motion. This leads immediately to the significance of a new quantity known as *isobaric spin.*

TABLE 5.1 Parameters of the two-nucleon system

Parameter	*Value*/10^{-15} m			*Method of determination*
	(np)	(pp)	(nn)	
Triplet scattering length a_t	$5{\cdot}425 \pm 0{\cdot}0014$	—	—	Low-energy (np) scattering Coherent scattering
Singlet scattering length a_s	$-23{\cdot}714 \pm 0{\cdot}013$	$-7{\cdot}821 \pm 0{\cdot}004$*	$-17{\cdot}4 \pm 1{\cdot}8$	Low-energy (np) and (pp) scattering Coherent scattering Final state interactions
Triplet effective range r_{0t}	$1{\cdot}749 \pm 0{\cdot}008$	—	—	Binding energy of deuteron Photodisintegration
Singlet effective range r_{0s}	$2{\cdot}73 \pm 0{\cdot}03$	$2{\cdot}830 \pm 0{\cdot}017$	$2{\cdot}4 \pm 1{\cdot}5$	Low-energy (np) and (pp) scattering Capture of slow neutrons by protons Final state interactions

* The proton–proton scattering length becomes about 17 fm when correction is made for the Coulomb forces.

5.6 Isobaric (isotopic) spin (Ref. 1.1a, p. 87)

5.6.1 Formalism

The neutron and proton have a similar mass and identical spin and, as has just been seen, apparently participate similarly in mutual interactions so long as Coulomb effects are disregarded and so long as the pair of interacting particles is in the same quantum state. It was therefore proposed as early as the 1930s and soon after the discovery of the neutron, that the two particles might be regarded as two states of a single particle, the *nucleon*, distinguished simply by the label of charge. Since electromagnetic forces are weak compared with nuclear forces within the range of the nuclear interaction, the disturbance of this simplifying assumption by charge-dependent effects should be small.

To describe this in symbols suitable for quantum calculations it is useful to start by drawing an analogy with the quantum theory of angular momentum. It is well known that a state with angular momentum $\boldsymbol{J}$ has $2J+1$ substates J_z which become distinct in a finite magnetic field. Similarly, an intrinsic spin has $2s+1$ orientations with respect to an axis of quantization, and for $s=\frac{1}{2}$ this indicates two states. The two states of the nucleon can, therefore, be described by assigning a fictitious vector $\boldsymbol{T}$ with quantum number $T=\frac{1}{2}$ to the basic particle and by regarding the proton and neutron as substates with $T_z=+\frac{1}{2}$ and $T_z=-\frac{1}{2}$ respectively. These substates become distinct once the underlying symmetry is broken by Coulomb effects, i.e. by the recognition of charge. Because of the close analogy with intrinsic spin the new quantity is known as *isobaric* or *isotopic spin* (*i*-spin) although it has nothing to do with ordinary mechanical variables. Like intrinsic spin, it exists only in virtue of the assumption of a symbolic space in which it can assume permitted orientations. In each orientation the charge state is specified by the component T_z. The value of this formal description is that it may easily be extended to systems of particles and that it facilitates the expression of a new conservation law.

The discussion of conserved quantities in Section 1.3 emphasizes their connection with symmetries and with the fact that the corresponding operator commutes with the Hamiltonian operator H. Thus, for ordinary angular momentum $\boldsymbol{J}$ the Hamiltonian is invariant under rotations of the coordinate system in ordinary space and

$$[H, \boldsymbol{J}]=0 \tag{5.47}$$

so that $\boldsymbol{J}$ is conserved in an isolated system. Convenient commuting operators are then $\boldsymbol{J}^2$ and $\boldsymbol{J}_z$ with eigenvalues given by

$$\left.\begin{aligned} \boldsymbol{J}^2\psi &= J(J+1)\hbar^2\psi \\ \boldsymbol{J}_z\psi &= J_z\psi = M\hbar\psi \quad \text{with} \quad |M|\leqslant J \end{aligned}\right\} \tag{5.48}$$

where ψ is a wavefunction in ordinary space. And for isobaric spin, we now postulate that the Hamiltonian operator is invariant under rotations in the fictitious *i*-spin space. In analogy with (5.47) and (5.48) we then have, omitting the angular momentum $\hbar$,

$$[H, \boldsymbol{T}] = 0 \tag{5.49}$$

$$\left.\begin{aligned} \boldsymbol{T}^2\phi &= T(T+1)\phi \\ \boldsymbol{T}_z\phi &= T_z\phi \qquad |T_z| \leqslant T \end{aligned}\right\} \tag{5.50}$$

where ϕ is a wavefunction in *i*-spin space and T is the isobaric spin quantum number. The inference from (5.49) that T_z is a constant of the motion expresses the *conservation of charge*, which is a well-known experimental fact, but the conclusion that $\boldsymbol{T}^2$ is constant, i.e. that *total isobaric spin is conserved* is new and is a generalization of the charge independence hypothesis. It means that the strong interaction between particles depends on $\boldsymbol{T}$ but not on T_z.

A simple illustration of the isobaric spin formalism in classifying particle states is found in the two-nucleon system discussed in this chapter. This system comprises the three possibilities (pp), (np) and (nn). By the rules for addition of quantum vectors, the total isobaric spin quantum number may be $T = T_1 + T_2 = 1$ or 0. The third component, measuring total charge, must be $T_z = 1, 0, -1$ in the three cases, and each of these is a substate of the state with $T = 1$. Moreover, the (np) system, with $T_z = 0$, is also a substate of total *i*-spin $T = 0$. It can now be seen immediately that the two-nucleon singlet states have $T = 1$, i.e.

$$^1\mathrm{S}_0 \qquad \mathrm{pp}\ (\mathrm{np})_{\mathrm{singlet}}\ (\mathrm{nn}) \qquad T = 1,\ T_z = 1, 0, -1 \tag{5.51a}$$

and the two-nucleon triplet state occurs only with $T = 0$, i.e.

$$^3\mathrm{S}_1 \qquad (\mathrm{np})_{\mathrm{triplet}} \qquad T = 0,\ T_z = 0 \tag{5.51b}$$

In this particular case of two similar particles such as nucleons, with isospin $\frac{1}{2}$, there is no mixing of isospin states for a given state of motion, e.g. $^1\mathrm{S}_0$ or $^3\mathrm{S}_1$. The validity of total isospin as a good quantum number is then directly equivalent to charge independence of the nuclear force, i.e. that the interaction is the same in all similar states of motion (e.g. $^1\mathrm{S}_0$) with the same T (e.g. 1) but different T_z and is different from that in states of other T (e.g. 0). A more restrictive possibility is that the interaction is the same for the same T and $|T_z|$, i.e. for (pp) and (nn), but different for (np) which has $T_z = 0$. This would be the result of charge symmetry of the nuclear force.

In a state of $T = 1$, but not of $T = 0$, a neutron or proton may be changed to the other particle without offending the exclusion principle. The *i*-spin concept thus permits a useful generalization of the Pauli principle; permitted states of two nucleons are those which have antisymmetrical wavefunctions for exchange of *all* coordinates, i.e. isobaric spin, ordinary spin and position. Thus, the two-nucleon state $T=1$, $^1S_0$ is symmetrical in i-spin, antisymmetric in ordinary spin and symmetrical in space coordinates.

We may extend this discussion to the levels of complex nuclei, under the reasonable assumption that these are determined by interactions for which charge independence is valid. For the nucleons, we note that the particle charge Q may be expressed in units of $|e|$ as

$$Q=(T_z+\tfrac{1}{2}) \tag{5.52}$$

and for a nucleus containing N neutrons and Z protons with $N+Z=A$, the third component of total i-spin is

$$T_z=(Z-N)\tfrac{1}{2}=(A-2N)\tfrac{1}{2}=(2Z-A)\tfrac{1}{2} \tag{5.53}$$

whence

$$Q=Z=(T_z+A/2) \tag{5.54a}$$

In elementary-particle language this would be written

$$Q=(T_z+B/2) \tag{5.54b}$$

using B the baryon number in place of A. This expression, and also (5.52), relates to non-strange particles and may be generalized to include both strangeness and charm as shown in Table 2.2.

Since from (5.50) $|T_z|\leqslant T$, the total isobaric spin for a nuclear state in a nucleus with known T_z (i.e. known charge Z) must have $T\geqslant|T_z|$. A level of known T, e.g. 1, will therefore be expected to occur in $(2T+1)$ isobaric nuclei, though not at the same excitation in all because of the corrections necessary for neutron–proton mass difference and Coulomb repulsion. Figure 5.9 shows an isobaric triad for $A=10$. (Odd-mass mirror nuclei such as ^{13}C, ^{13}N provide many examples of isobaric doublets.)

In Fig. 5.9*b* the $(0^+, T=1)$ level of ^{10}B is the isobaric analogue of the ground state of ^{10}Be. Such states are also found in much heavier nuclei, and at much greater excitation because of the increasing Coulomb energy of the proton-richer isobar. The analogue state may then, in many cases, be excited directly by a proton-induced nuclear reaction, and the reaction yield as a function of proton energy shows a characteristic feature known as an *isobaric analogue resonance.*

Isobaric spin conservation is found experimentally to be valid generally for the strong interaction (Ch. 11) apart from violations due to electromagnetic forces. Two illustrations are given in the following section.

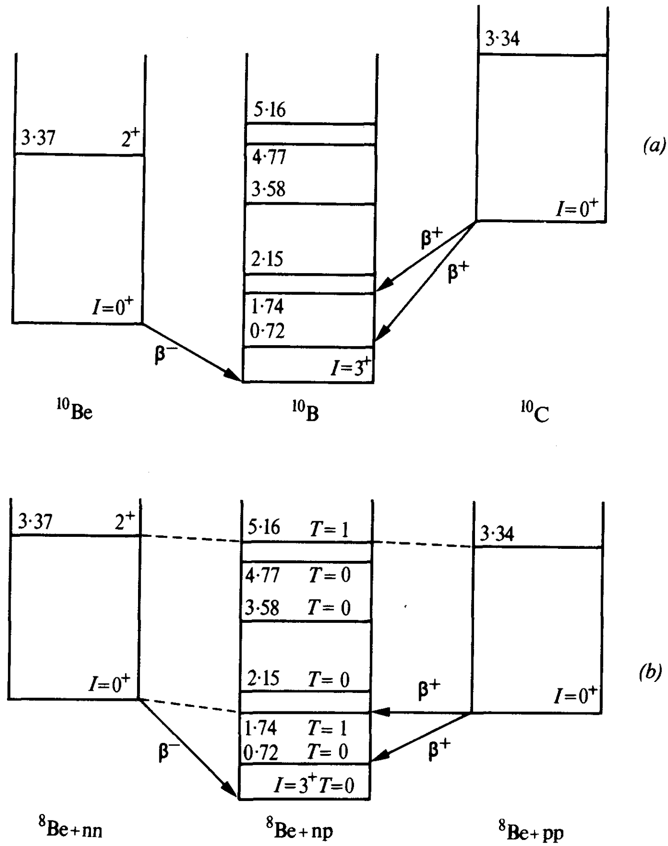

Fig. 5.9 Low-lying levels of the isobars of mass 10. Energies are marked in MeV and spins and parities are indicated by the symbols 0^+, 1^+, etc. (*a*) Masses of bare nuclei. (*b*) Nuclear masses corrected for Coulomb energy and for neutron–proton mass difference, showing isobaric triplet levels.

5.6.2 Application to scattering problems

(i) *Nucleon–nucleon scattering.* Proton–proton collisions take place in a state of pure isobaric spin $T=1$ because $T=T_z=\frac{1}{2}$ for each particle. Only the partial waves for the states ^{1}S, ^{3}P, ^{1}D, . . . are allowed to contribute to the scattering amplitude as noted in Section 5.3.1.

The s-wave neutron–proton collision has been analysed so far in terms of singlet (^{1}S) and triplet (^{3}S) spin states with relative weights of 1 and 3 (eqn (5.17)). From the discussion in Section 5.6.1 it follows that these spin states are pure states of $T=1$ and $T=0$

respectively. If the scattering cross-section is to be analysed in terms of isobaric spin eigenstates, however, it must be remembered that only one of the $T=1$ triplet of states is accessible to the (np) system, namely that with $T_z=0$. This system must, therefore, be considered to be equally in the $T=1$ and $T=0$ states. Charge independence apart from Coulomb effects exists between the $T=1$ substates, but not between the (pp) state and the complete mixed (np) system.

Figure 5.7 gives the variation of the proton–proton cross-sections over a range of energies for which several partial waves are important, although their number is limited by centrifugal barrier penetration effects. From this information and from similar data for the (np) system the variation of the $T=1$ and $T=0$ cross-sections over the same energy range can be extracted. Differential cross-sections for the (pp) (Fig. 5.8) and (np) (Fig. 5.3) interactions have also been obtained over a wide range of energies, and together with the elastic cross-sections and some observations of spin-polarization effects provide the data from which phase-shift analyses up to about 400 MeV laboratory energy may be made; beyond this extra parameters are needed to deal with the inelastic channels.

The phase shifts, two of which are plotted in Fig. 5.4, join smoothly with the low-energy values δ_{0s}, δ_{0t} discussed in Section 5.2.2. The $^1S_0$ phase shift ($T=1$ state) becomes negative at about 250 MeV and this is evidence for a repulsive core in the nucleon–nucleon interaction at a radius of about 0·5 fm, as assumed in Section 5.1. Altogether, the phase shifts summarize a large body of experimental data and can be used for testing potential models of the nucleon–nucleon interaction.

The (np) differential cross-section at energies of about 100 MeV is nearly symmetric about 90° c.m. and the depth of the 90° dip increases with energy. The high intensity of neutrons apparently scattered through 180° (c.m.) cannot be understood if the (np) well depth is only about 30 MeV as indicated by the low-energy experiments, because the whole of the neutron energy has been transferred to the proton. If, however, the proton and neutron can change their identity in the collision, then a backward neutron peak can occur for low momentum transfer. This phenomenon is known as *charge exchange scattering* and is evidence for an *exchange behaviour* in the nucleon–nucleon force. The forward peak in the scattering cross-section is due to the ordinary, non-exchange scattering.

(ii) *Pion–proton scattering.* The pion (Sect. 2.2.1) is an isobaric triplet, that is to say it has $T=1$ and three charge states with $T_z=1$, 0, -1 corresponding with π^+, π^0 and π^- particles. The total isobaric spin number for the (πp) system is, therefore, $T=\frac{3}{2}$ or $\frac{1}{2}$ with $T_z=\frac{3}{2}$, $\frac{1}{2}$, or $-\frac{1}{2}$, of which the first is found only in the $T=\frac{3}{2}$ state. Experimentally, differential cross-sections have been measured for the elastic scattering processes

$$\pi^+ + p \rightarrow \pi^+ + p \tag{5.55}$$

$$\pi^- + p \rightarrow \pi^- + p \tag{5.56}$$

and for the charge-exchange process

$$\pi^- + p \rightarrow \pi^0 + n \tag{5.57}$$

For process (5.55) the pion–nucleon system is an eigenstate of isobaric spin with $T=\frac{3}{2}$, $T_z=\frac{3}{2}$ and if charge independence is valid should have the same cross-section as (π^-n) scattering, with $T=\frac{3}{2}$, $T_z=-\frac{3}{2}$. These cross-sections would also be equal to those for other pion–nucleon states such as (π^-p), (π^+n), (π^0p) and (π^0n) if these belonged wholly to the $T=\frac{3}{2}$ multiplet. This, however, is not so, because the T_z values in these cases permit a mixture of $T=\frac{1}{2}$ states and the pion–nucleon states must be represented by the proper superpositions of eigenstates of T, T_z. This situation differs from that discussed for the two-nucleon system because the interacting particles are now not identical and the different T values do not necessarily imply different space–spin states (e.g. ^{3}S, ^{1}S).

The expansion of a product wavefunction $\phi(\text{pion}) \times \phi(\text{nucleon})$ in terms of eigenstates of T, T_z may be obtained directly from the table of Clebsch–Gordan or vector coupling coefficients for the case labelled $j_1=1$, $j_2=\frac{1}{2}$ given in Appendix 4. The m-values in the table are the T_z-values for the pion and nucleon concerned. The same table enables an eigenstate of T, T_z (labelled J, M) to be decomposed into a sum of products of pion and nucleon states. Thus, for the (π^-p) system with a T_z of $-1+\frac{1}{2}=-\frac{1}{2}$ we have

$$\phi(\pi^-p) = \phi_1(\pi^-)\phi_2(p) = \sqrt{\tfrac{1}{3}}\,\psi(\tfrac{3}{2}, -\tfrac{1}{2}) - \sqrt{\tfrac{2}{3}}\,\psi(\tfrac{1}{2}, -\tfrac{1}{2}) \tag{5.58}$$

Also, the eigenstate $\psi(\frac{3}{2}, -\frac{1}{2})$ may be related to the pion–nucleon systems with the same T_z of $-\frac{1}{2}$, namely, (π^-p) and (π^0n):

$$\psi(\tfrac{3}{2}, -\tfrac{1}{2}) = \sqrt{\tfrac{1}{3}}\,\phi(\pi^-p) + \sqrt{\tfrac{2}{3}}\,\phi(\pi^0n) \tag{5.59}$$

These and similar formulae permit the hypothesis of conservation of isobaric spin in the pion–nucleon interaction to be tested by predicting the ratio of cross-sections for the processes (5.55), (5.56) and (5.57).

Let the (angle-dependent) scattering amplitude be $f_{3/2}$ for the $T=\frac{3}{2}$ state and $f_{1/2}$ for the $\frac{1}{2}$ state, each independent of T_z in accordance with charge independence within a T-multiplet. Then in the (π^+p) scattering the incident state $\phi(\pi^+p)$ is the i-spin state $\psi(\frac{3}{2}, \frac{3}{2})$ and leads simply to a final state with the same (conserved) i-spin but including a factor $f_{3/2}$.

For (π^-p) scattering, however, the initial state is mixed in i-spin, as shown in (5.58) above and an i-spin conserving interaction leads to a final state containing the wavefunction

$$\sqrt{\tfrac{1}{3}}f_{3/2}\psi(\tfrac{3}{2},-\tfrac{1}{2})-\sqrt{\tfrac{2}{3}}f_{1/2}\psi(\tfrac{1}{2},-\tfrac{1}{2}) \tag{5.60}$$

This can be put back into pion × nucleon states using expressions such as (5.59) and the result is

$$(\tfrac{1}{3}f_{3/2}+\tfrac{2}{3}f_{1/2})\phi(\pi^-\text{p})+\left(\frac{\sqrt{2}}{3}f_{3/2}-\frac{\sqrt{2}}{3}f_{1/2}\right)\phi(\pi^\circ\text{n}) \tag{5.61}$$

from which we conclude that the elastic scattering amplitude, process (5.56), is $(\frac{1}{3}f_{3/2}+\frac{2}{3}f_{1/2})$ and the charge exchange amplitude, process (5.57), is $\sqrt{2}/3(f_{3/2}-f_{1/2})$.

This is, so far, only descriptive, but if now it is assumed that for a particular energy the amplitude $f_{1/2}$ happens to be small (e.g. in the neighbourhood of the $\Delta(1236)$ resonance which has $\text{T}=\frac{3}{2}$), then the differential cross-sections for the three reactions at any angle should stand in the ratio $(\frac{1}{3})^2:(\sqrt{2}/3)^2:1$, i.e. $1:2:9$. This is, in fact, verified to an encouraging degree of precision, and the result lends important support to the hypothesis of the conservation of isobaric spin in this hadronic interaction.

More detailed examination of the extensive body of data that now exists permits the scattering amplitudes $f_{3/2}$ and $f_{1/2}$ to be obtained over a wide range of energy involving a series of partial waves. Their variation as a function of c.m. energy displays peaks at the mass values of nucleon isobars, e.g. the $\Delta(1236)$. They are normally expressed in terms of relativistically invariant variables, and may be analysed to yield a value for the pion–nucleon coupling constant (Sect. 2.3).

5.7 Electromagnetic properties of the deuteron; non-central forces

5.7.1 Neutron–proton capture and photodisintegration

The processes of thermal neutron capture

$$\text{n}+\text{p}\rightarrow\text{d}+\gamma \tag{5.62}$$

and its inverse, photodisintegration

$$\gamma+\text{d}\rightarrow\text{n}+\text{p} \tag{5.63}$$

exchange energy between the neutron–proton system and an electromagnetic field. The minimum exchange is the binding energy of the deuteron and process (5.62) indeed yields the most accurate value of this quantity:

$$\varepsilon = 2{\cdot}2245\pm0{\cdot}0002\ \text{MeV}$$

The spins of the particles concerned (n, p $=\frac{1}{2}$ and d $=1$) allow each of the processes to occur by a magnetic dipole interaction, e.g. $^1S \rightarrow {}^3S$ for capture and $^3S \rightarrow {}^1S$ for photoeffect. The intrinsic spins 'flip' in this process and the angular momentum change $1\hbar$ is conveyed to or from the photon. The coupling between the nucleons and the electromagnetic field is via the intrinsic magnetic moments and the cross-sections in the zero-range approximation include a factor $(\mu_p - \mu_n)^2$. There is also a factor $(1-\alpha a_s)^2$, where α is the deuteron size parameter and a_s is the singlet scattering length, and this makes the cross-section sensitive to the sign of this latter quantity. The observed value of the capture cross-section confirms that the ^1S state of the deuteron is unbound (a_s negative).

The photodisintegration process (5.63) may also take place through the electric dipole transition $^3S \rightarrow {}^3P$ and this is responsible for the major part of the total cross-section except very near threshold, where the magnetic transition dominates because the emission of p-wave particles is retarded by a centrifugal barrier-penetration factor. The photoelectric cross-section reaches a maximum at a photon energy $h\nu \approx 2\varepsilon$ and is then of the order of magnitude of the 'area' of the deuteron $\pi/4\alpha^2$ multiplied by the fine structure constant, which represents the coupling to the electromagnetic field. The cross-section in zero-range approximation can readily be corrected for finite range and then contains a factor $(1-\alpha r_{0t})^{-1}$ from which the triplet effective range may be extracted.

5.7.2 *Magnetic and electric moments; tensor and spin-orbit forces*

The magnetic moment of the deuteron in units of the nuclear magneton $\mu_N = e\hbar/2m_p$ is less than the sum of the intrinsic magnetic moments of the neutron and proton, taken to be parallel for the ^3S configuration:

$$\mu_d = 0{\cdot}857\,411 \pm 0{\cdot}000\,019 \qquad \begin{aligned} \mu_n &= -1{\cdot}913\,15 \pm 0{\cdot}000\,07 \\ \mu_p &= 2{\cdot}792\,71 \pm 0{\cdot}000\,02 \\ \mu_n + \mu_p &= 0{\cdot}879\,56 \pm 0.000\,07 \end{aligned}$$

The closeness of the two values confirms that the magnetic moment of the neutron is negative, but it is not possible to explain the difference if the two particles are in a pure s-state of relative motion. Moreover, such a state is spherically symmetrical and has no electric moments, whereas the deuteron is known to have a positive electric quadrupole moment (Sect. 3.4.1) of $0{\cdot}29\,\mathrm{fm}^2$ corresponding with an elongation of the density distribution along the spin axis.

These facts can be explained if the deuteron wavefunction contains a d-state component, indicating some motion of the two particles with a relative *orbital* angular momentum quantum number of 2. The D-state consistent with the observed spin of the deuteron is $^3D_1$ and the ground state wavefunction would then be written

$$\psi(\mathrm{SD}) = a\psi(^3\mathrm{S}) + b\psi(^3\mathrm{D}) \tag{5.64}$$

where the mixing is to be produced by an appropriate property of the internucleon potential. If the mixing coefficient is expressed by the perturbation theory formula

$$b/a = \int (\psi_\mathrm{D}^* |V| \psi_\mathrm{S})\, \mathrm{d}^3 r/(E_\mathrm{D} - E_\mathrm{S}) \tag{5.65}$$

where E_D and E_S are the energies of pure D- and pure S-states, then it can immediately be seen that if V is of a purely radial nature, i.e. if the force is purely central, the matrix element vanishes because of orthogonality of ψ_D and ψ_S. In other words, central forces do not mix states of different angular momentum, whereas equation (5.65) requires a force for which $\boldsymbol{L}^2$ is *not* a constant of the motion if b is to be finite.

A suitable non-central interaction is provided by adding a *tensor* component V_T to the potential. This may be written

$$V_T = V_T(r) S_{12} \tag{5.66}$$

where

$$S_{12} = 3(\boldsymbol{s}_\mathrm{p} \cdot \boldsymbol{r}_\mathrm{p})(\boldsymbol{s}_\mathrm{n} \cdot \boldsymbol{r}_\mathrm{n})/\mathrm{r}^2 - (\boldsymbol{s}_\mathrm{p} \cdot \boldsymbol{s}_\mathrm{n}) \tag{5.67}$$

and s_p, s_n are the spin vectors divided by $\hbar$. This gives a velocity-independent force depending on the relative orientation of the spin vectors and the line joining the particles (Fig. 5.10); it resembles the classical interaction between magnetic dipoles. Detailed calculations show that if about 7 per cent of the ground state wavefunction is D-state and if $V_T < 0$ then the electromagnetic moments of the deuteron are correctly predicted.

Tensor forces are not effective in singlet states because there is no preferred spin axis. It might, therefore, be possible to ascribe the whole of the spin dependence of nuclear forces to the existence of non-central effects in the triplet state, and a tensor-type interaction is indeed suggested by meson-exchange theories. The existence of spin polarization effects in nucleon scattering and the theory of nuclear shell structure (Ch. 7), however, jointly require the existence of a coupling between spin and orbital motion of a single nucleon in a potential field. Such a force in a complex nucleus may derive from a two-body *spin-orbit* force between a pair of nucleons with a potential

$$V_{LS} = V_{LS}(r) \boldsymbol{L} \cdot \boldsymbol{S} \tag{5.68}$$

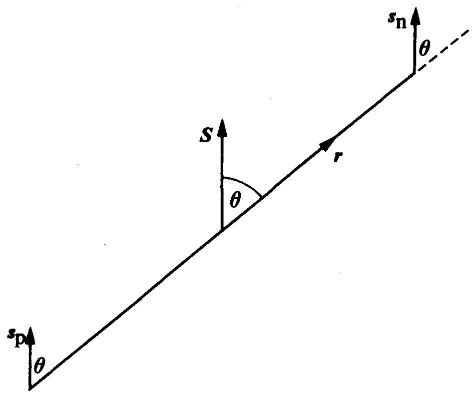

Fig. 5.10 Spin vectors in the (triplet) ground state of the deuteron (spin **S**). The minimum energy for the tensor force is when $\theta = 0$ or 180°. The deuteron is then cigar-shaped, with a positive quadrupole moment.

Such a force does not mix states of different L (because $\boldsymbol{L}\cdot\boldsymbol{S}/\hbar^2$ is a number (cf. Ex. (7.4)) and cannot account for the properties of the deuteron.

5.8 Summary and theoretical description

From the evidence presented in this chapter it appears that the force between nucleons has the following properties:

(*a*) short range (≈ 2 fm);
(*b*) spin dependence;
(*c*) charge symmetry and most probably charge independence to a good approximation except for electromagnetic effects;
(*d*) an exchange behaviour;
(*e*) a repulsive core of radius $\approx 0{\cdot}5$ fm in the ^{1}S state and probably also in other states of motion, and an attractive potential outside the core in the ^{1}S and ^{3}S states at least;
(*f*) a tensor and a spin-orbit term in addition to the central forces.

The potential energy function for the central part of the force is typically as shown in Fig. 5.1.

The meeting-point between experiment and theory in the discussion of the nuclear force is the comparison between observed and calculated two-nucleon phase shifts. Many *phenomenological potentials* (Hamada–Johnston, Yale University, Tabakin) that predict the phase shifts have been proposed. In addition to conforming with the requirements summarized above, they are constrained by the general invariance principles relating to space translation or rotation, parity and time reversal (Sect. 1.3). A general type of potential may be written

$$V = V_C + V_{CS} + V_{LS} + V_T + V_{QLS} \tag{5.69}$$

where V_C is the spin-independent central potential;
V_{CS} is the spin-dependent central potential;
V_{LS} is the two-body spin-orbit potential;
V_T is the tensor potential;
V_{QLS} is a quadratic spin-orbit potential (which will not be discussed).

Each potential term in (5.69) has a radial dependence determined by the range of the force, and contains operators for spin, isospin, position and momentum which give the necessary properties (cf. (5.67) and (5.68)). Thus, the isospin operators give a potential depending on total isospin rather than its third component (charge independence) and can be used to describe a force arising from the exchange of charge between a neutron and proton. Similarly, the spin operators can be arranged to describe forces arising from the exchange of spin, and the spin–isospin operators jointly describe forces connected with change of position.

The several types of exchange force that are formally described in this way were originally introduced (by Heisenberg) to account for the saturation of the force (Sect. 5.1) because some of the exchange forces have opposite signs in even and odd angular momentum states. A repulsive core, of course, also contributes to a saturation requirement, but the evidence of (np) scattering (Sect. 5.6.2) makes it clear that exchange characteristics must be included in the general potential.

The phenomenological potentials leading to attractive forces have well depths of $\approx$1000 MeV at the hard-core radius. Since the deuteron binding energy is only 2·2 MeV, it follows that the strength of the forces is only just sufficient to produce a bound state, and that this arises from the long-range part of the force.

Both ordinary and exchange forces are predicted if a meson is literally *exchanged* between the interacting particles, as shown in Fig. 2.8. As pointed out by Yukawa, the short range of the force is a consequence of the finite mass of the exchanged particle, and the range $\hbar/\mu c$, with $\mu = m_\pi$ thus indicated (Sect. 2.2.1) agrees well with observation. The attractive one-pion exchange potential (OPEP) calculated in this way has several of the features of the phenomenological potential (5.69), particularly charge independence, tensor and exchange properties. The OPEP deals only with the 'long-range' part of the force; to include the shorter distances and especially the repulsive core, more complex exchanges are required in addition, especially of two pions and of ω, ϕ and ρ particles.

Realistic potentials should be used in nuclear matter and nuclear structure calculations but formidable difficulties arise because of the singular nature of the 'hard' repulsive core. One way in which these difficulties have been circumvented, in the case of nuclear matter, is outlined in Section 6.4. For nuclear structure, simplified forms of the potential may be used with considerable success in predicting the sequence of low-lying excited states once the basic single-particle states have been established. An example will be given in Section 8.6.

Examples 5

5.1 Using the tabulated values of the magnetic moment of the neutron and proton, calculate the force between these two particles in a triplet state at a separation of 3×10^{-15} m, and calculate the work required, on account of this force, to bring the neutron from infinity to this distance from the proton. Assume that the spins always point along the line joining the particles. [1 N, 6267 eV]

5.2* Estimate the range of the repulsive core of the nucleon–nucleon potential given that the s-wave ($^1S_0$) phase shift vanishes for a laboratory energy of 250 MeV.

5.3 Using $r_{0t} = 1{\cdot}75$ fm, find the correction to the triplet scattering length introduced by the effective range term in equation (5.32). [1·1 fm]

5.4 Using equation (5.19) and writing $k = i\alpha$ for the bound state, deduce the relation (5.32). You may assume that $i\delta_0$ is a large quantity, which is required if the external wavefunction is to be well behaved at infinity (Ref. 6.4).

5.5* Assuming that the wavefunction $u(r) = r\psi(r) = Ce^{-\alpha r}$ is valid for the deuteron from $r = 0$ to $r = \infty$, obtain the value of the normalization constant C.

If $\alpha = 0{\cdot}232\ \mathrm{fm}^{-1}$ find the probability that the separation of the two particles in the deuteron exceeds a value of 2 fm.

Find also the average distance of interaction for this wavefunction.

5.6 Suppose that the deuteron is represented by a square-well potential of depth 20 MeV and radius 2·5 fm. Plot the effective potential for $l = 1$ and $l = 2$ states and comment on the possibility of the formation of a bound state.

5.7 A particle of kinetic energy T and mass M is scattered by a square-well potential of radius a and depth b. Show that the s-wave phase shift for $k \to 0$ is given by

$$\tan \delta_0 = k \tan k'a/k' - \tan ka$$

where

$$k^2\hbar^2 = 2MT, \qquad (k')^2\hbar^2 = 2M(T+b)$$

5.8 The triplet and singlet scattering lengths for the neutron–proton system are 5·4 fm and 23·7 fm respectively. Calculate the elastic scattering cross-section expected for neutrons of energy 1 eV. [20·3 b]

5.9 Using the principle of isospin conservation, predict the ratio of the total cross-sections for the reactions $p+p \to d+\pi^+$ and $n+p \to d+\pi^0$ as far as isospin factors are concerned. [2/1]

5.10 Using the $1, \frac{1}{2}$ table of Appendix 4 write down a complete list of pion–nucleon states in terms of eigenstates of isospin. Write down also the expression of the isospin eigenstates in terms of pion–nucleon states.

5.11 The total cross-section for (Λp) scattering at $T = 10$ MeV (c.m.) is 100 mb. Assuming that the singlet and triplet scattering lengths are each $-1{\cdot}7$ fm, find the effective range, also assumed the same in singlet and triplet states. [3·09 fm]

What is the physical meaning of a negative scattering length in both states?

5.12* Using equation (1.77), write down the elastic scattering amplitude for the (np) system at an energy at which only s- and p-waves are effective and inelastic processes may be disregarded. Neglecting terms of second order in δ_1, find the differential cross-section and show that if δ_1 is positive $\sigma(180°) < \sigma(0°)$ whereas for δ_1 negative $\sigma(180°) > \sigma(0°)$. (A repulsive force in odd-parity states is characteristic of the *Majorana* type of exchange force.)

5.13* By expressing two-nucleon states in terms of states of pure isospin, show that the integrated elastic cross-section in the state $T=0$ at a given energy is $\sigma_{T=0} = 2\sigma_{np} - \sigma_{pp}$.